2021-03

Galleria mellonella larvae exhibit a weight-dependent lethal median dose when infected with methicillin-resistant Staphylococcus aureus

Hesketh-Best, PJ

1 *Galleria mellonella* **larvae exhibit a weight-dependent lethal**

2 **median dose when infected with Methicillin-resistant**

3 *Staphylococcus aureus*

4 **Authors**

5 Poppy J. Hesketh-Best[1*], Michelle V. Mouritzen[2], Kayleigh Shandley-Edwards[1],

6 Richard A. Billington[1], and Mathew Upton[2]

7 [1]School of Biological and Marine Sciences, and [2]School of Biomedical Sciences,

8 University of Plymouth, PL4 8AA UK.

9 * Corresponding author: Poppy J. Hesketh Best

10 (poppy.heskethbest@plymouth.ac.uk)

11 **Abstract**

12 *Galleria mellonella* is a recognised model to study antimicrobial efficacy; however,

13 standardisation across the scientific field and investigations of methodological

14 components are needed. Here we investigate the impact of weight on mortality

15 following infection with Methicillin-resistant *Staphylococcus aureus* (MRSA). Larvae

16 were separated into six weight groups (180-300 mg at 20 mg intervals) and infected

17 with a range of doses of MRSA to determine the 50% lethal dose (LD_{50}), and the

18 'lipid weight' of larvae post-infection was quantified. A model of LD_{50} values

19 correlated with weight was developed. The LD_{50} values, as estimated by our model,

20 were further tested *in vivo* to prove our model.

21 We establish a weight-dependent LD_{50} in larvae against MRSA and demonstrate that

22 *G. mellonella* is a stable model within 180-260 mg. We present multiple linear

23 models correlating weight with: LD_{50}, lipid weight, and larval length. We demonstrate

24 that the lipid weight is reduced as a result of MRSA infection, identifying a potentially

25 new measure in which to understand the immune response. Finally, we demonstrate

26 that larval length can be a reasonable proxy for weight. Refining the methodologies

27 in which to handle and design experiments involving *G. mellonella*, we can improve

28 the reliability of this powerful model.

32   **Introduction**

33   *Galleria mellonella* (Greater wax moth) larvae are widely utilised for toxicity

34   screening (Desbois and Coote 2012; Maguire, Duggan and Kavanagh 2016; Coates

35   *et al.* 2019) and to study host-pathogen interactions (Peleg *et al.* 2009; Olsen *et al.*

36   2011; Junqueira 2012; Wojda and Taszłow 2013). Unlike many insect models, *G.*

37   *mellonella* can be incubated at 37°C, which facilitates the investigation of human

38   pathogens. This has included most of the ESKAPE pathogens: *Enterococcus*

39   *faecium* (Chibebe Junior *et al.* 2013; Luther *et al.* 2014); *Staphylococcus aureus*

40   (Brackman *et al.* 2011; Ramarao, Nielsen-Leroux and Lereclus 2012; Sheehan,

41   Dixon and Kavanagh 2019); *Klebsiella pneumoniae* (Wand *et al.* 2013; Diago-

42   Navarro *et al.* 2014); *Acinetobacter baumannii* (Peleg *et al.* 2009); and

43   *Pseudomonas aeruginosa* (Jander, Rahme and Ausubel 2000; Seed and Dennis

44   2008). Additionally, *Escherichia coli* (Leuko and Raivio 2012; Alghoribi *et al.* 2014;

45   Jønsson *et al.* 2017; Guerrieri *et al.* 2019)*, Bulkholderia mallei* (Schell, Lipscomb and

46   DeShazer 2008) and several fungi (Cotter, Doyle and Kavanagh 2000; Reeves *et al.*

47   2004; Mylonakis *et al.* 2005) have also been studied using *G. mellonella*. Crucially, a

48   positive correlation between the virulence and immune responses between

49   mammalian models and *G. mellonella* has been established for *P. aeruginosa*

50   (Jander, Rahme and Ausubel 2000), *Cryptococcus neoformans* (Mylonakis *et al.*

51   2005), and *S. aureus* (Sheehan, Dixon and Kavanagh 2019)*,* demonstrating the

52   powerful potential of this invertebrate model.

53   Antibiotic efficacy at dosages recommended for human use can be tested in *G.*

54   *mellonella*, in addition to their toxicity correlating with toxicity observed in murine

55   models (Ignasiak and Maxwell 2017). This has been shown with both natural and

56   synthetic compounds (Gibreel and Upton 2013; Smitten *et al.* 2019), opening up the

57   possibility of a rapid and cheap model for the early stages of discovery and

58   development of natural and synthetic products, without the challenges of ethical

59   approval, specialist training and the difficulties of using mice-models in early-stage

60   drug development. Infections caused by antibiotic-resistant *S. aureus* are of global

61   concern and it is listed as a high priority pathogen for which new antibiotics are
62   urgently needed (The World Health Organisation 2017). Methicillin-resistant *S.*
63   *aureus* (MRSA) has been utilised with *G. mellonella* for the study of virulence
64   (Mannala *et al.* 2018), pathogenicity (Ebner *et al.* 2016), antimicrobial efficacy of
65   existing antimicrobials (Ba *et al.* 2015; Ferro *et al.* 2016), and for novel candidates
66   (Gibreel and Upton 2013; Jacobs *et al.* 2013; Dong *et al.* 2017) (Table S1).

67   Despite the increased popularity of *G. mellonella*, there is much variability in method
68   application (Andrea, Krogfelt and Jenssen 2019). This includes differences in larval
69   size, storage, infective dose, and injection intervals. In this study, we address larval
70   size and its potential impact in experimental design. In antibiotic efficacy studies,
71   typically the model is infected with a pathogen shortly before the candidate treatment
72   is presented. This has not been standardised with respect to the parameters
73   previously mentioned for *G. mellonella*. In our preliminary experimentation in
74   determining a 50% lethal dose (LD_{50}) for MRSA in *G. mellonella*, it was noted that
75   smaller larvae were more susceptible to infection than larger larvae. This was when
76   using a broad range of larval weights (~200-300 mg), as previously reported (Jacob*s*
77   *et al*. 2013). Furthermore, the larval weight has been demonstrated to positively
78   correlate with the larval liquid volume, leading to recommendations on how *in vivo*
79   concentrations of injected compounds and pathogens should be calculated (Andrea,
80   Krogfelt and Jenssen 2019). This led us to hypothesise that the larvae LD_{50} for a
81   pathogen, in our case here MRSA, is directly proportional to the larvae weight and
82   that larvae weight is an essential parameter in experimental design that must be
83   tightly controlled.

84   When physical and anatomical barriers are breached, the wax moth larvae have an
85   innate immune response relying on germline-encoded factors for the detection and
86   clearance of microbial pathogens (Trevijano-Contador and Zaragoza 2019). There
87   are two branches, cellular and humoral immunity. Cellular immunity is conducted by
88   haemocytes, which are present in an open circulatory system called the
89   haemolymph, which is analogous to vertebrate blood. There are at least six
90   subpopulations of haemocytes which perform similar roles to those of the myeloid
91   lineage in vertebrates (Boman and Hultmark 1987; Lavine and Strand 2002), and
92   they are also associated with digestive system, trachea and fat body (Ratcliffe 1985).
93   Five types of haemocytes were identified in fifth larval instar of *G. mellonella*;

94   prohaemocytes, plasmatocytes, granulocytes, oenocytoids and spherulocytes

95   (Salem *et al.* 2014).The main immune processes include coagulation, phagocytosis

96   and encapsulation (Tojo *et al.* 2000). Circulating haemocyte density increases during

97   pathogenesis due to the release of suspended cells from the fat body (Tojo *et al.*

98   2000). Haemocyte density and subpopulation variations changes with time of

99   exposure to pathogen and pathogen virulence (Arteaga Blanco *et al.* 2017).

100   Melanisation additionally occurs in the haemolymph, the process of melanin

101   production resulting in the darkened appearance of the larvae (Tojo *et al.* 2000). The

102   humoral branch is involved in the production of lytic enzymes (Vogel *et al.* 2011),

103   and antimicrobial peptides (AMPs) that are active against bacterial pathogens

104   (Cytryńska *et al.* 2007; Tsai, Loh and Proft 2016). These molecules are mostly

105   produced by the larval 'fat body', analogous to the mammalian liver, and are

106   released into the haemolymph (Zasloff 2002).

107   A proteomic investigation has shown *S. aureus* infections lead to an increase in

108   production of proteins such as AMPs and peptidoglycan recognition proteins

109   (Sheehan, Dixon and Kavanagh 2019). Critically, the same study identified

110   similarities between *G. mellonella* and mammal immune response to *S. aureus*

111   infections. What has not been investigated is the physiological change in *G.*

112   *mellonella* lipid as a result of *S. aureus* infections. For this investigation, we were

113   motivated to quantify the lipid weight, a proxy for the fat body, of the larvae to

114   observe how the fat body might have been affected as a result of MRSA infection.

115   The aim of the work here is to investigate methodological adjustments which may

116   improve the reproducibility and reliability of using pet-food grade *G. mellonella* as an

117   experimental model. This was achieved by (i) examining the effect of larval weight on

118   the LD_{50} to MRSA infection, and (ii) characterising physiological changes occurring

119   to lipid weight as a result of the larval immune response to MRSA.

120   **Materials and Methods**

121   *Cultivation of MRSA*

122   A single colony of Methicillin-resistant *Staphylococcus aureus* (MRSA) NTCT 12493

123   was streaked onto fresh Luria broth (LB, Fischer Scientific, UK; Tryptone 10 g/L,

124   yeast extract 5 g/L, and sodium chloride 10 g/L) solidified with 1.5% agar (Acros

125 Organics, UK) 24 h before experimentation. Single colonies were suspended in

126 Dulbecco A Phosphate buffered saline (PBS, Oxoid UK) to a range of optical density

127 (OD) read at 600 nm (Eppendorf BioPhotometer, Netherlands). These dilutions were

128 OD_{600} = 0.1 - 1.0 in 0.1 increments. Viable cell counts were made of each dilution.

129 *Determining a weight-based LD$_{50}$ for* Galleria mellonella *larvae*

130 Larvae were purchased commercially from Livefoods UK Ltd. (Somerset, UK;

131 www.livefoods.co.uk). On receipt, larvae were individually weighed using an

132 accurate scale and grouped into the following weight bands: 180-200, 201-220, 221-

133 240, 241-260, 261-280, and 281-300 mg. Larvae were stored at 4°C for up to 7 days

134 in the dark with no food and water. Healthy larvae were identified by a uniform cream

135 colour, with no indications of melanisation such as spots or markings (Fig. 1A) (Li *et*

136 *al.* 2018). Larvae were euthanised by chilling them at 4°C for 1 h, before freezing

137 them at -20°C for a minimum of 24 h.

138
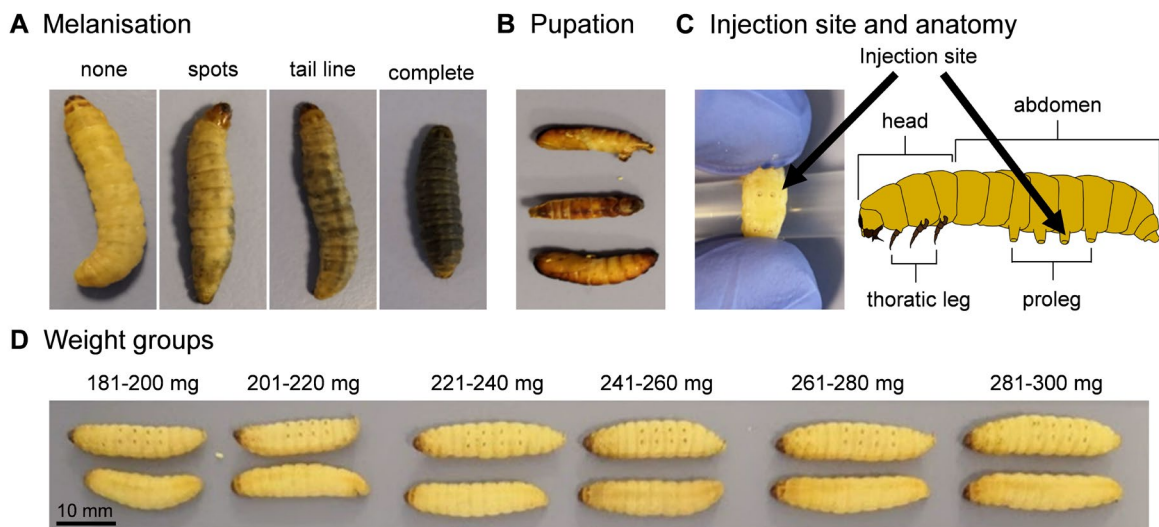
Figure 1: *Galleria mellonella* larvae. (A) Melanisation is a visual indication of the health of the larvae, as larvae progress from none to complete melanisation as a result of stress and/or infection. (B) Larvae pupation. (C) Route of infection for larvae is by intra-haemocoelic injection at the penultimate pro-leg (arrow). Larvae diagram was adapted from Singkum *et al.* (2019). (D) Larvae are divided up into six weight groups.

144 Larvae (n = 10) from each weight band were infected by injecting 10 µl of one of the

145 10 dilutions of MRSA into the left penultimate pro-leg (Fig. 1C), using a 50 µl

146 Hamilton 750 syringe (Hamilton Company, UK) with a removable needle. Injected

147 larvae were placed into Petri dishes lined with tissue paper (KIMTECH, UK). Three

148 independent replicates of this experiment were carried out. Syringes were cleaned

149 before and after each bacterial dilution. Cleaning consisted of taking up and

150 discarding of each wash solution thrice before progressing to the next wash solution.

151 Wash solution order was as follows: distilled H_2O (dH_2O), 70% ethanol, and dH_2O.

152 After infection, the larvae were maintained at 37°C in the dark without food or water.

153 A placebo control of sterile PBS was used to account for the effect of the physical

154 trauma of injection, along with a non-manipulation (NM) control. After 24 h the

155 live/dead counts were recorded. Larvae were recorded as dead when they met the

156 following: (i) complete melanisation (Fig. 1A), (ii) did not respond to touch, and (iii)

157 could not correct itself when rolled onto its back.

158 Determining the weight-dependent LD_{50}, live/dead counts were converted into

159 percentage mortality at 24 h for each group. For this investigation we have defined

160 LD_{50} as CFU of MRSA per mg of organism resulting in 50% mortality. To model the

161 dose-response and describe the relationship between increasing the infection dose

162 on survival for each weight group, a non-linear sigmoidal regression curve was

163 plotted. The infection dose, represented as CFU/ mg of total weight of larva, was log-

164 transformed. A non-linear regression curve was calculated to fit best the data

165 generated from three independent replicas. From the equation generated from this

166 curve, the theoretical LD_{50} was calculated along with the standard deviation (SD).

167 Estimated LD_{50} from each weight groups were plotted against the mean larvae

168 weight. A regression line was drawn, and the coefficient of determinant R^2 was

169 calculated.

170 *Correlating larval size with rate of pupation*

171 On the day of receipt, larvae were placed into weight groups in Petri dishes. They

172 were immediately placed at 37°C, in the dark with no food or water and permitted to

173 pupate over 15 days. Larvae were observed daily and pupation events recorded.

174 *Quantifying lipid weight of* G. mellonella

175 Following investigation of the LD_{50} for MRSA, the lipid weight for all living and dead

176 larvae was quantified. Live larvae from treatments, the NM and PBS controls were

177 ethically euthanised. Dead larvae were stored at -20°C until needed. Larvae were left

178 to thaw at room temperature for 24 h and were weighed and individually placed in

179   Eppendorf tubes to be dried over 7 days at 55°C, and re-weighed to reveal their dry

180   weight. Larvae were then submerged in ≥99.9% diethyl ether (Sigma-Aldrich, UK)

181   and left for 3 days at 4°C to dissolve lipid. Diethyl ether was utilised as the lipid

182   extraction solvent (Tzompa-Sosa *et al.* 2014). After, ether was left to evaporate in a

183   fume hood for 24 h. Once dried, larvae were weighed again to acquire the post-ether

184   weight. Quantities are then presented as followed: 'total weight' is the weight of the

185   larvae pre-experimentation; 'water weight' ($water\ weight =$

186    $pre\text{-}experimentation\ weight - dry\ weight$); 'lipid weight' ($lipid\ weight =$

187    $dry\ weight - post\text{-}ether\ weight$).

188   *Statistical analysis*

189   All statistical analysis was performed using PRISM GraphPad 8.4.2 (GraphPad

190   Software, San Diego, CA, USA). One-Way ANOVA (two-tailed), Two-Way ANOVA,

191   and Pearson's correlation coefficients were used when applicable to compare

192   treatment groups. Log-rank Mantel-Cox tests compared survival curves for

193   antimicrobial efficacy tests and pupation. A *p*-value of: < 0.05 ($*$), < 0.01 ($**$) or $<$

194   0.001 ($***$), < 0.0001 ($****$) was considered to be significantly different.

195   **Results**

196   *Larval weight affects LD$_{50}$*

197   To begin testing our hypothesis, LD$_{50}$ values were determined for each weight group.

198   A sigmoidal non-linear model best fit the dose-dependent response of the data,

199   resulting in an LD$_{50}$ calculated for each weight group (Fig. 2). When adjusted to the

200   number of cells injected into each larvae per one unit of body weight (CFU/mg), the

201   resulting LD$_{50}$ ranged from 1.19×10^{7}CFU/mg, for the 180-200 mg group, to the

202   highest LD$_{50}$ which was 8.97×10^{7} CFU/mg for the 261-280 mg group (Table 1). The

203   LD$_{50}$ increased across weight groups except for the 281-300 mg group, which had a

204   lower LD$_{50}$ than the 261-280 mg weight group. Throughout this experiment, we

205   encountered some difficulties when handling larvae from the two higher weight-

206   bands (261-280 and 281-300 mg), such as high variation in mortality at the lowest

207   infective dosages (0-40% mortality) and highest dosages (60-100% mortality).

208   Nevertheless, we were able to calculate an LD$_{50}$ with the final data.
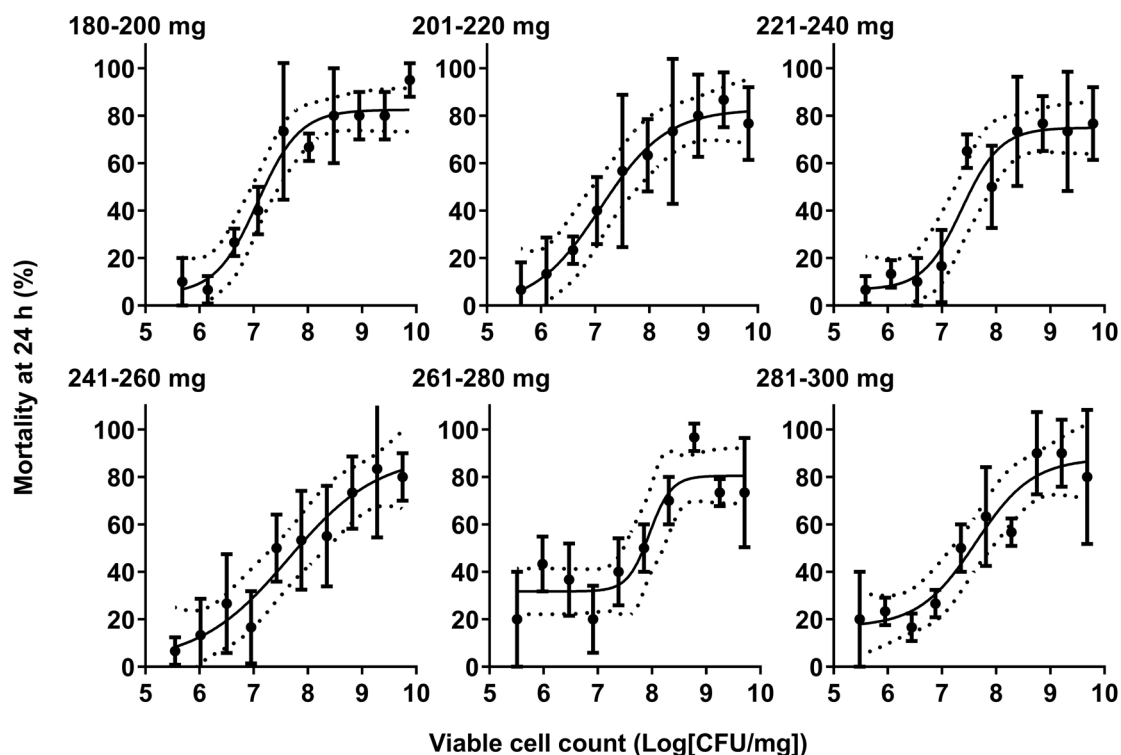
Figure 2. Sigmoidal non-linear logistic regressions best fit the dose-dependent response observed when calculating an LD_{50} for MRSA. LD_{50} was calculated for each weight group with 10 larvae/group. Data are shown as mean ± SD (n = 10) of three independent replicas.

Table 1. Summary of the LD_{50}s as calculated by non-linear models for each weight group (N, number of replicas; R^2, coefficient of determination).

Weight group (mg)	LD_{50} (CFU/mg][a]	SD (CFU/mg)	N	R^2
180-200	1.19×10^7	1.47	30	0.85
201-220	1.26×10^7	2.45	30	0.77
221-240	2.34×10^7	1.57	30	0.80
241-260	4.40×10^7	3.35	30	0.76
261-280	8.97×10^7	1.46	30	0.69
281-300	4.19×10^7	1.81	30	0.78

[a]Example of how this is calculated can be found in Table S3

We observed a positive correlation between weight of the larvae and LD_{50}, as calculated by Pearson correlation test (r = 0.87, *p* = 0.025, n = 18). A linear regression model arriving at an equation ($y = 0.007966x + 5.548$) was used to estimate LD_{50} (Fig. 3A). The LD_{50} values, as estimated by our model, were tested *in*

223   *vivo*, demonstrating an approximate 50-56% (± 5.7 – 10%) survival for four of the

224   weight groups (Fig. 3B). Survival at 24 h for the weight groups 261-280 and 281-300

225   mg was 30% (± 0%) and 43% (±15.3%), respectively.
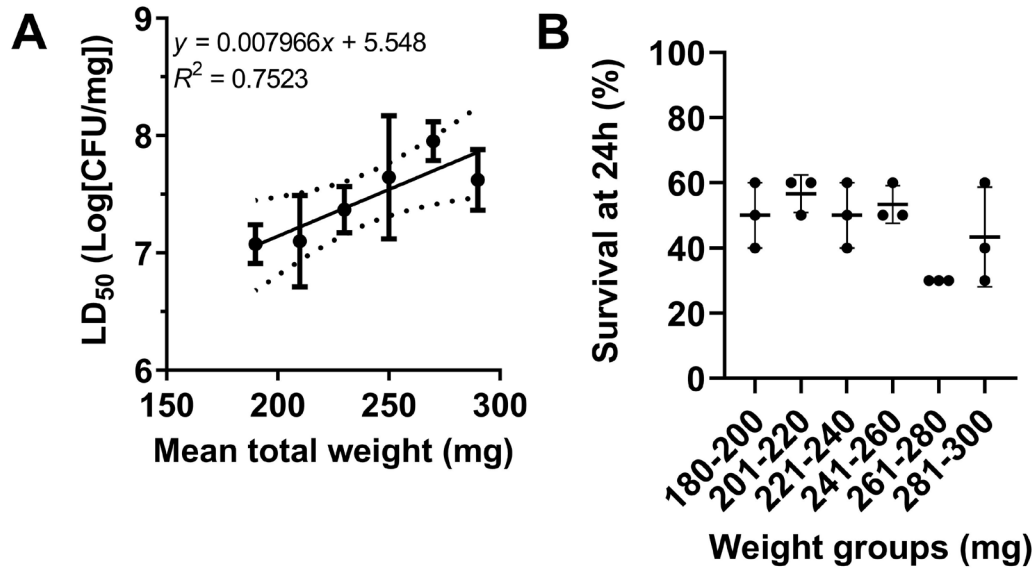
226

227   **Figure 3.** LD_{50} as calculated by non-linear regression models positively correlated with weight and
228   was validated *in vivo* for all but the two highest weight groups. (A) Calculated LD_{50} by non-linear
229   models correlation positively with total weight. (B) LD_{50} value as calculated by the model was
230   validated by injecting into larvae and observing mortality. Data are shown as mean ± SD (n=10) of
231   three independent replicas.

232   *MRSA infection leads to a reduction in lipid weight*

233   With the non-manipulated (NM) group, we assessed the overall relationship between

234   total weight, dry weight, and lipid weight and length of the larvae (Fig. 4). Determined

235   by Pearson's correlation test, we found a positive correlation between the total and

236   dry weight, (r = 0.972, *p* < 0.0001, n = 83) (Fig. 4A), and total and water weight (r =

237   0.989, *p* < 0.0001, n = 83) (Fig. 4B). These two results support the findings of

238   previous research (Andrea, Krogfelt and Jenssen 2019). Two additional positive

239   correlations were observed between total weight and lipid (r = 0.788, *p* < 0.0001, n =

240   83) (Fig. 4C), and total weight and length (r = 0.9944, *p* < 0.0001, n = 252) (Fig. 4D).
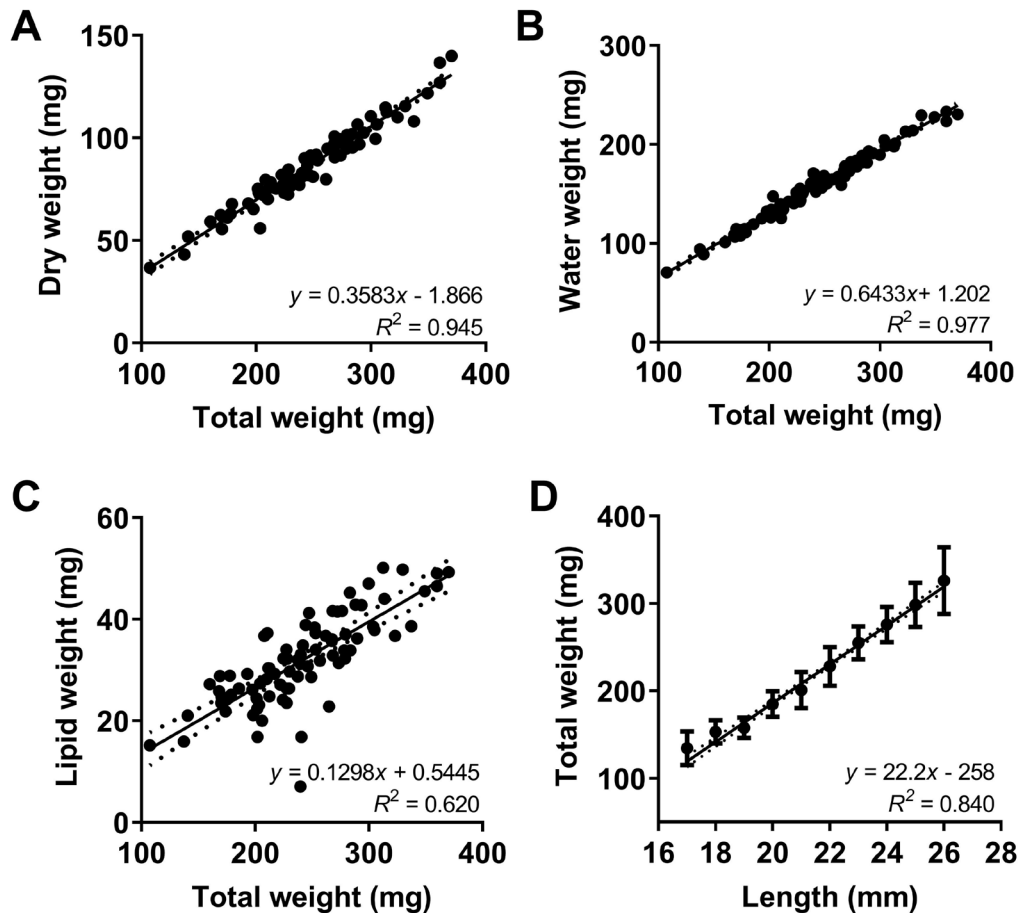
Figure 4. Multiple correlations observed between larvae total weight and dry weight, water weight, lipid weight, and larvae length. Non-manipulated (NM) larvae were used to analyse the relationships between (A) total weight and dry weight, (B) total weight and the lipid weight after here presented as lipid weight, (C) total weight and lipid weight as proportional to the total weight, water weight, and (D) total weight and larvae length where data is presented as mean ± SD (n = 252).

We also investigated the effect of infection on the lipid weight of all the larvae used in determining the LD_{50} for MRSA (Fig. 5). As calculated by one-way ANOVA, injection with MRSA resulted in an overall decrease in the lipid weight for both dead (18.7 mg ± 8.541, p < 0.0001, n = 573) and live larvae (22.4 mg ± 6.556, p < 0.0001, n = 524), when compared to the NM control (31.92 mg ± 8.815, n = 83) (Fig 5A). When compared to one another, live larvae had a significantly greater lipid weight compared to dead larvae (*p* <0.0001). There was no significant reduction in the lipid weight between NM and PBS control (27.81 mg ± 5.825, *p* > 0.999, n = 50) (Fig 5A and Table S2).
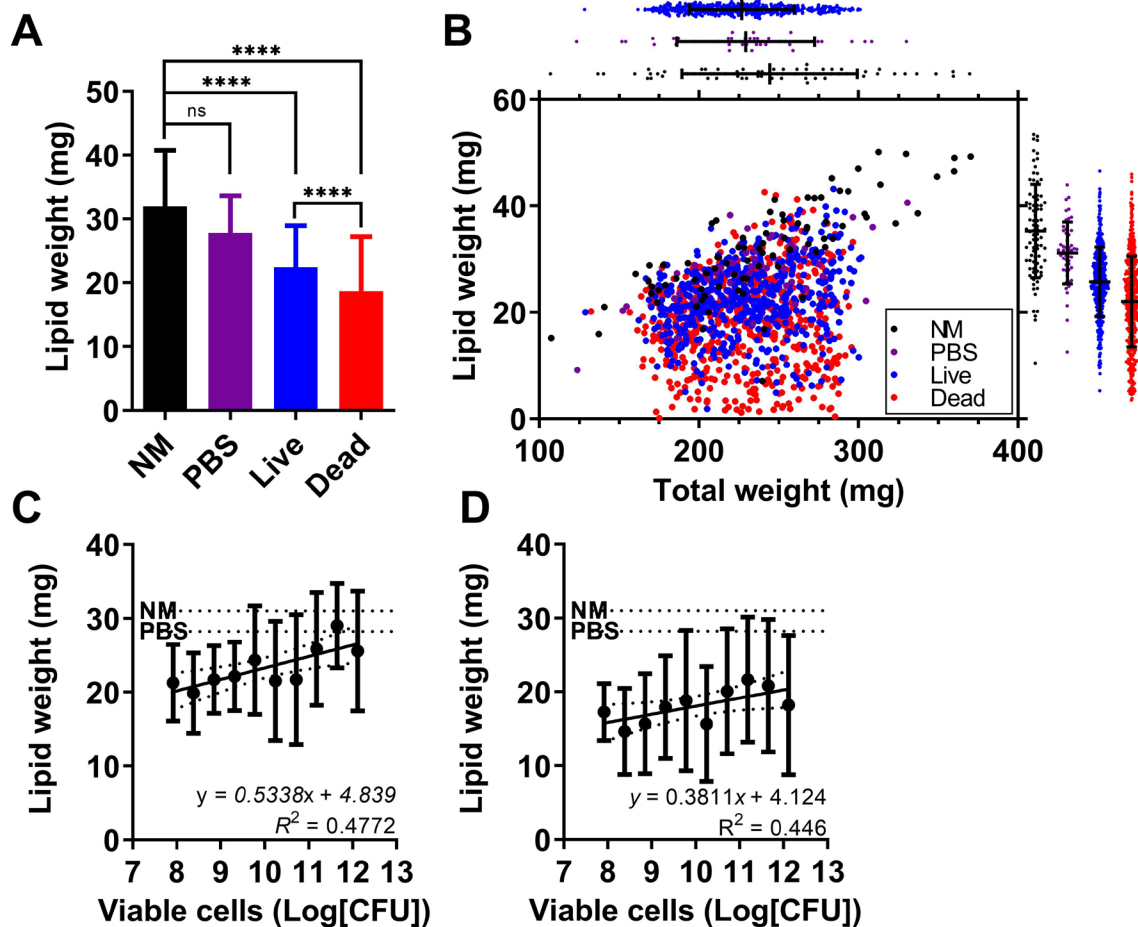
Figure 5. Injection of the larvae with MRSA results in an overall decreased in the lipid weight of the larvae. (A) Statistical results from a one-way ANOVA are illustrated above the bars as compared to the NM control. Summary of multiple analysis can be found in Table S2. (B) Box-plots above and to the right of the scatter plot are to illustrate the distribution of the data. Colours are as follows: black, NM control; purple, PBS control; blue, live larvae; and red, dead larvae 24 h post-MRSA infection. Correlations of infective dose and lipid weight for (C) living and (D) dead larvae. Data is presented as Log[CFU], as the infective doses are not adjusted for larvae weight. Data presented as mean ± SD (n = 10) of three independent replicas.

Finally, we observed that at a high infective dosage of MRSA, the larvae had a lipid weight close to the mean of the NM and PBS control compared to the lower dosages (Fig. 5C-D). This was supported by a positive correlation between lipid weight and infective dose for both live (r = 0.778, p = 0.008) (Fig. 5C) and dead larvae (r = 0.669, p = 0.035) (Fig. 5D).

Pupation is unaffected by weight

274   To explore whether larger larvae were closer to the final instar stage (pupae) in
275   which they begin to pupate into adult moths, an observational experiment was
276   performed. NM larvae were left to pupate at 37°C, and it was observed that 80-100%
277   of larvae pupated within the 15 day incubation period, independent on their weight
278   grouping, as calculated by Log-rank (Mantel-Cox) test (X^2(5, N = 60) = 4.004, p =
279   0.549) (Fig. 6).
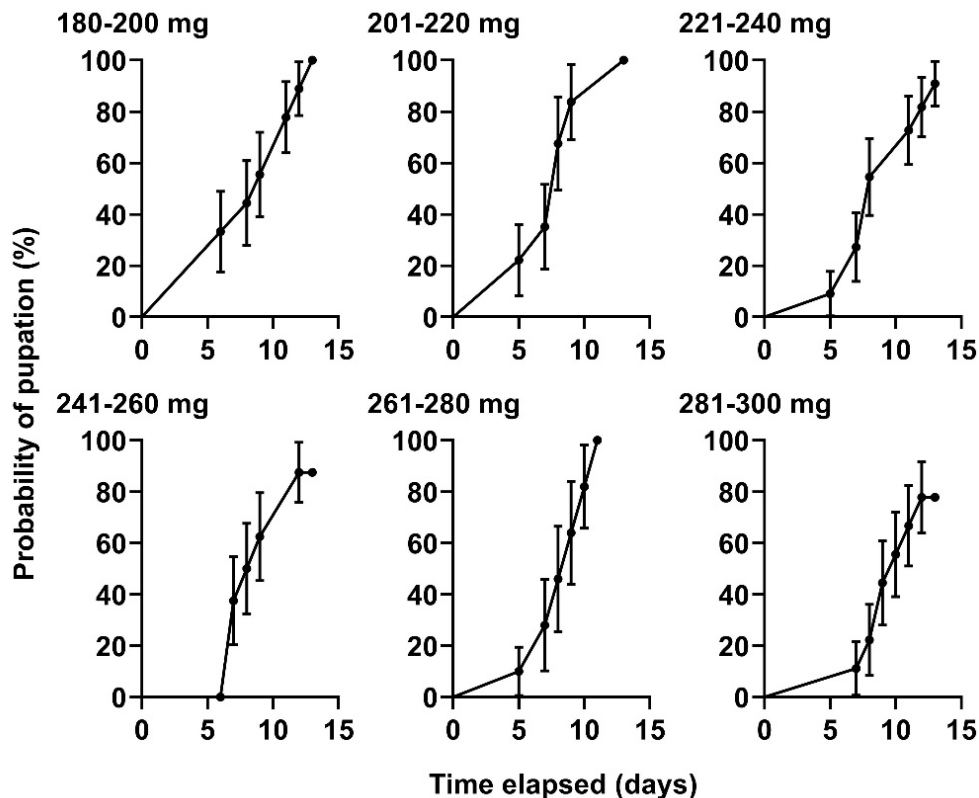
280

281   **Figure 6.** The weight did not influence the probability of pupation of NM larvae. NM larvae
282   were incubated at 37°C for 15 days and observed daily for pupation events. No significant
283   difference was found between the weight group and the probability of pupation as calculated
284   by a Log-rank Mantel-Cox test (p = 0.5489). Data are shown as mean ± SD (n = 10)
285   repeated twice.

286 **Discussion**

287 *MRSA exhibits a weight-dependent LD_{50}*

288   In this study, we have demonstrated it is possible to develop a model in which a LD_{50}
289   can be predicted based on the weight of the larvae, and that the prediction can be
290   experimentally validated (Fig. 3). The linear model correlating total and water weight
291   (Fig. 4B) imply that in increasingly larger larvae, the *in vivo* dilution of MRSA
292   increases requiring a greater density of pathogen to reach the LD_{50}. Likewise for the

293   positive correlation confirmed with total and lipid weight (Fig. 4C), the presence of a

294   larger fat body that can be degraded for the production of immune factors, may well

295   be why we observe the weight-dependent effect on LD_{50}. The LD_{50}s (1.19 – 8.97

296    $x10^7$ CFU/mg) for the MRSA strain was not within range of infective dosages utilised

297   in previously investigated MRSA and Methicillin-sensitive *S. aureus* (MSSA) strains

298   (0.8 – 5.0 $x10^6$ CFU) (Table S1). However, a direct comparison may not be

299   appropriate given the variation in reporting densities as in our study the LD_{50} was

300   adjusted to account for *in vivo* dilution in the larvae as described in Andrea, Krogfelt

301   and Jenssen (2019), but this is not always done.

302   During the process of this investigation, we found two of the largest weight groups

303   (261-280 and 281-300 mg) to be unreliable, which hindered progress. This was

304   consistent across multiple batches of larvae orders. LD_{50}, as calculated by our model

305   for 261-280 and 281-300 mg larvae, resulted in less than 50% survival at 24 h (Fig.

306   3B), indicating that our model for a weight-dependent LD_{50} had overestimated the

307   LD_{50}. Our first assumptions were that larger larvae were older and closer to pupation

308   than the smaller weight groups, as larvae increase in size until pupation (Jorjão *et al.*

309   2018), which might somehow impact on survival. Given the difficulty in identifying an

310   age for each larva, it is a difficult hypothesis to test beyond quantifying the number of

311   days it took for NM larvae from each weight group to pupate.

312   When this was conducted, we found that larval size did not influence the probability

313   of pupation (Fig. 6), and we conclude that the larvae received from the supplier had

314   an 80-100% probability of pupating within 15 days if kept at 37°C, regardless of

315   weight. It would appear that larger larvae were not likely to be closer to pupation than

316   smaller ones, so the reason for our observed decrease in LD_{50} for large larvae

317   remains unknown. Since larvae were kept without food, this may be a reason for the

318   observed similar pupation times across all weight groups as lack of food source may

319   be forcing the larvae into pupation. Feeding regimes are not the standard protocol

320   when investing antibiotic efficacy, as such we feel this best represented the

321   conditions larvae would be exposed to at the start of experimentation.

322   Using *G. mellonella* does have drawbacks, one such being the functional equivalent

323   of adaptive immunity termed 'immune priming' (Little and Kraaijeveld 2004; Sadd

324   and Schmid-Hempel 2006). Individual larvae that survive infection or exposure to a

325   particular pathogen may exhibit increased immune resistance against the same or

326   similar pathogens. Priming with heat-killed pathogens was observed to result in

327   increased larval survival (Wu *et al.* 2014). Ultimately there will be no control over the

328   immune history of the larvae and this should always be recognised when working

329   with pet-food grade *G. mellonella.* Across the literature, a wide range of weight

330   bands have been utilised: 150-200 mg (Mannala *et al.* 2018); 300-700 mg (Ebner *et*

331   *al.* 2016); 200-300 mg (Jacobs *et al.* 2013); and in other studies this is not declared

332   (Ba *et al.* 2015; Jorjão *et al.* 2018). Our results suggest that choosing weight ranges

333   as wide as 300-700 mg and 200-300 mg could result in inconsistent data. While a

334   weight range of only 20 mg is likely a conservative approach, ranges such as 100

335   mg or greater in our weight-dependent LD_{50} model for MRSA indicates that there

336   would be significant differences in survival (Fig. 3A).

337   Weighing individual larvae is a time-consuming procedure. This study also

338   demonstrated that larvae length is reasonable proxy for the weight (Fig. 4D). Larval

339   length has been previously used to characterise larvae for experimentation where

340   larvae of 15-25 mm were utilised (Bazai*d et al*. 2018). Like total weight, a large

341   length grouping may also encounter similar challenges. A 20 mg weight grouping

342   would equate to roughly 1 mm, for example, 180-200 mg would be 20-21 mm.

343   Measuring length may be a preferred alternative to accurately weighing all larval.

344   When sourcing larvae from our supplier, we frequently found that larvae belonging to

345   the weight groups 201-220 and 221-240 mg were most abundant, which will

346   inevitably be the practical determining factor in weight group selection. Our findings

347   would support selection of larvae in this range.

348   *Lipid metabolism occurs in response to MRSA infection*

349   MRSA infection leads to a decreased lipid weight in the larvae after 24 h, whether

350   they died or survived the infection (Fig. 5A). The reduction in lipid weight is likely the

351   result of lipolysis during an immune response. This is to be expected, the fat body of

352   the larvae produce many defence compounds essential to the larvae's immune

353   response (Cytryńska *et al.* 2007; Tsai, Loh and Proft 2016). This reaction can be

354   rapid, in some models showing production of AMPs within the first 4 to 6 h post-

355   infection (Sheehan, Dixon and Kavanagh 2019; Trevijano-Contador and Zaragoza

356   2019). This is supported by proteomic work, which demonstrated that at 6 and 24 h

357   post-*S. aureus* infection larvae had increased expression of AMPs (Sheehan, Dixon
358   and Kavanagh 2019).

359   On exposure to the infecting pathogen, there may be a rapid metabolism of the fat
360   body to provide the required energy to fight the infection. Larvae with larger lipid
361   weight before infection might be more likely to survive, as seen with the surviving
362   larvae having a greater lipid weight than dead larvae (Fig. 5A). Within this
363   experimental design, the larvae are not fed before or during the experiment, and
364   therefore they cannot be acquiring more lipid. Where lipid weight was seen as closer
365   to the NM and PBS control baseline, as observed in the trend of lipid weight
366   positively correlating with infective dose (Fig. 5C-D), it is more likely that lipid
367   metabolism has been compromised.

368   What could reasonably be expected is that lipolysis of the fat body occurs to
369   increase the production of AMPs and additional defence compounds. When
370   *Drosophila* are stimulated by a systemic infection with *S. aureus*, signalling from the
371   Toll receptor increases, which leads to increased production of AMPs and reduced
372   accumulation of lipids (Liu *et al.* 2016; Lee and Lee 2018). This could suggest that
373   for larvae surviving high infective dosages, there are additional immune responses
374   that do not deplete the fat body.

375   We intended to quantify the larval lipid weight to aid in understanding the weight-
376   dependent LD_{50} effect and the observed unreliability of the two largest weight groups
377   (261-280 and 281-300 mg). We report several observations regarding the lipid
378   weight and MRSA infection; however, none can fully explain the irregularity we
379   encountered for the largest weight groups. Analysing larval lipid weight has proved
380   some insight, but would benefit from further investigation, though alternative
381   methods to estimate lipid mass would be required.

382   *Overall assessment of* G. mellonella *as a model*

383   There remains a lack of widely available and cheap standardised stocks of larvae
384   reared under controlled conditions. Temperature (Mowlds and Kavanagh 2008), diet
385   (Banville, Browne and Kavanagh 2012; Jorjão *et al.* 2018), past infections (Fallon,
386   Kelly and Kavanagh 2012), and antibiotics and hormones in the feed (Büyükgüzel
387   and Kalender 2008) are all reported to influence laboratory experimentation. Most

388   larvae currently used are acquired from commercial insect food providers (Andrea,

389   Krogfelt and Jenssen 2019), where it is understood that use of antibiotics and

390   hormones in the culture medium is common practice, and acquiring accurate

391   information regarding the conditions in which the larvae are reared is challenging. All

392   of which may vary between larvae suppliers, which is a challenge that warrants

393   further investigation.

394   Ultimately from our investigation, it would appear that lipid deposits are essential in

395   *G. mellonella* response to MRSA. Prior investigation has evaluated the effect of

396   nutrient deprivation on larvae (Banville, Browne and Kavanagh 2012), and the

397   selection of diet (Jorjão *et al.* 2018), which both influence susceptibility to *S. aureus*

398   infection. This emphasises the issues associated with a having lack of knowledge of

399   rearing conditions used by suppliers and how they will influence experimental

400   results. TruLarv™ (BioSystems Technology, UK) currently provide the only

401   standardised *G. mellonella* in the UK. While cheap compared to murine models, it is

402   considerably costlier (£1.20 per larvae) than purchasing larvae from commercial pet

403   food providers.

404   However for pet-food grade larvae to be reliably used in research, more significant

405   consideration should be taken over the parameters that can be controlled, and in this

406   study, we emphasise that such experiments can be reproducible and reliable. We

407   recommend that investigators consider the potential variability associated with using

408   different larval weight as we have shown herein. We would recommend using weight

409   groupings as a means to control this. . Our data suggests that all larvae used should

410   be within 10 mg of the mean weight of all larvae to provide consistency. Additionally,

411   larvae of >260 mg should not be avoided.

412   In this work, we present several linear regression curves that could be used as tools

413   to aid in experimental design, such as the linear model for LD_{50} (Fig. 3A), weight and

414   lipid content (Fig. 4C), and length (Fig. 4D). Finally, we demonstrate that the lipid

415   weight is reduced as a result of MRSA infection, identifying a potentially new

416   measure in which to understand the immune response. Similarities between *G.*

417   *mellonella* and mammals in response to *S. aureus* infections can be used to study

418   the efficacy and interactions of novel antimicrobials, even at early development

419   stages. By refining and standardising methodologies in which to handle and select

420 *G. mellonella* for study, we can improve the reliability of this powerful model for
421 multiple purposes.

422 **Author Contributions**

423 Conceptualisation, PJHB and MVM; Methodology, PJHB, MVM, KSE, RAB, and MU;
424 Validation, PJHB, MVM, and KSE; Formal Analysis, PJHB; Investigation, PJHB and
425 MVM; Resources, PJHB and MVM; Data Curation, PJHB and MVM; Writing –
426 Original Draft Preparation, PJHB; Writing – Review & Editing, PHB, MVM, KSE,
427 RAB, and MU; Visualization, PJHB; Supervision, RAB, and MU; Funding Acquisition,
428 MU.

429 **Funding**

433 **Transparency declaration**

437 **References**

438 Alghoribi MF, Gibreel TM, Dodgson AR *et al. Galleria mellonella* infection model
439   demonstrates high lethality of ST69 and ST127 uropathogenic *E. coli. PLoS*
440   *One* 2014;**9**:e101547–e101547.

441 Andrea A, Krogfelt KA, Jenssen H. Methods and Challenges of Using the Greater
442   Wax Moth (*Galleria mellonella*) as a Model Organism in Antimicrobial
443   Compound Discovery. *Microorganisms* 2019;**7**:85.

444 Arteaga Blanco LA, Crispim JS, Fernandes KM *et al.* Differential cellular immune
445   response of *Galleria mellonella* to *Actinobacillus pleuropneumoniae. Cell Tissue*
446   *Res* 2017;**370**:153–68.

447 Ba X, Harrison EM, Lovering AL *et al.* Old drugs to treat resistant bugs: Methicillin-
448   resistant *Staphylococcus aureus* isolates with mecC are susceptible to a
449   combination of penicillin and clavulanic acid. *Antimicrob Agents Chemother*

450   2015;**59**:7396–404.

451   Banville N, Browne N, Kavanagh K. Effect of nutrient deprivation on the susceptibility

452   of *Galleria mellonella* larvae to infection. *Virulence* 2012;**3**:497.

453   Bazaid AS, Forbes S, Humphreys GJ *et al.* Fatty Acid Supplementation Reverses

454   the Small Colony Variant Phenotype in Triclosan-Adapted *Staphylococcus*

455   *aureus*: Genetic, Proteomic and Phenotypic Analyses. *Sci Rep* 2018;**8**, DOI:

456   10.1038/s41598-018-21925-6.

457   Boman HG, Hultmark D. Cell-free immunity in insects. *Annu Rev Microbiol*

458   1987;**41**:103–26.

459   Brackman G, Cos P, Maes L *et al.* Quorum sensing inhibitors increase the

460   susceptibility of bacterial biofilms to antibiotics in vitro and in vivo. *Antimicrob*

461   *Agents Chemother* 2011;**55**:2655–61.

462   Büyükgüzel E, Kalender Y. *Galleria mellonella* (L.) Survivorship, Development and

463   Protein Content in Response to Dietary Antibiotics. *J Entomol Sci* 2008;**43**:27–

464   40.

465   Chibebe Junior J, Fuchs BB, Sabino CP *et al.* Photodynamic and Antibiotic Therapy

466   Impair the Pathogenesis of *Enterococcus faecium* in a Whole Animal Insect

467   Model. *PLoS One* 2013;**8**:55926.

468   Coates CJ, Lim J, Harman K *et al.* The insect, *Galleria mellonella*, is a compatible

469   model for evaluating the toxicology of okadaic acid. *Cell Biol Toxicol*

470   2019;**35**:219–32.

471   Cotter G, Doyle S, Kavanagh K. Development of an insect model for the in vivo

472   pathogenicity testing of yeasts. *FEMS Immunol Med Microbiol* 2000;**27**:163–9.

473   Cytryńska M, Mak P, Zdybicka-Barabas A *et al.* Purification and characterization of

474   eight peptides from *Galleria mellonella* immune hemolymph. *Peptides*

475   2007;**28**:533–46.

476   Desbois AP, Coote PJ. Chapter 2 - Utility of Greater Wax Moth Larva (*Galleria*

477   *mellonella*) for Evaluating the Toxicity and Efficacy of New Antimicrobial Agents.

478   In: Laskin AI, Sariaslani S, Gadd GM (eds.). *Advances in Applied Microbiology*.

479   Vol 78. Academic Press, 2012, 25–53.

480 Diago-Navarro E, Chen L, Passet V *et al.* Carbapenem-resistant *Klebsiella*
481   *pneumoniae* exhibit variability in capsular polysaccharide and capsule
482   associated virulence traits. *J Infect Dis* 2014;**210**:803–13.

483 Dong CL, Li LX, Cui ZH *et al.* Synergistic effect of pleuromutilins with other
484   antimicrobial agents against *Staphylococcus aureus* in vitro and in an
485   experimental *Galleria mellonella* model. *Front Pharmacol* 2017;**8**:553.

486 Ebner P, Rinker J, Nguyen MT *et al.* Excreted cytoplasmic proteins contribute to
487   pathogenicity in *Staphylococcus aureus*. *Infect Immun* 2016;**84**:1672–81.

488 Fallon J, Kelly J, Kavanagh K. *Galleria mellonella* as a Model for Fungal
489   Pathogenicity Testing. *Methods Mol Biol* 2012;**845**:469–85.

490 Ferro TAF, Araújo JMM, dos Santos Pinto BL *et al.* Cinnamaldehyde Inhibits
491   *Staphylococcus aureus* Virulence Factors and Protects against Infection in a
492   *Galleria mellonella* Model. *Front Microbiol* 2016;**7**:2052.

493 Gibreel TM, Upton M. Synthetic epidermicin NI01 can protect *Galleria mellonella*
494   larvae from infection with *Staphylococcus aureus*. *J Antimicrob Chemother*
495   2013;**68**:2269–73.

496 Guerrieri CG, Pereira MF, Galdino ACM *et al.* Typical and Atypical
497   Enteroaggregative *Escherichia coli* Are Both Virulent in the *Galleria mellonella*
498   Model. *Front Microbiol* 2019;**10**:1791.

499 Ignasiak K, Maxwell A. *Galleria mellonella* (greater wax moth) larvae as a model for
500   antibiotic susceptibility testing and acute toxicity trials. *BMC Res Notes* 2017;**10**,
501   DOI: 10.1186/s13104-017-2757-8.

502 Jacobs AC, DiDone L, Jobson J *et al.* Adenylate kinase release as a high-
503   throughput-screening-compatible reporter of bacterial lysis for identification of
504   antibacterial agents. *Antimicrob Agents Chemother* 2013;**57**:26–36.

505 Jander G, Rahme LG, Ausubel FM. Positive correlation between virulence of
506   *Pseudomonas aeruginosa* mutants in mice and insects. *J Bacteriol*
507   2000;**182**:3843–5.

508 Jønsson R, Struve C, Jenssen H *et al.* The wax moth *Galleria mellonella* as a novel
509   model system to study Enteroaggregative *Escherichia coli* pathogenesis.

510   *Virulence* 2017;**8**:1894–9.

511   Jorjão AL, Oliveira LD, Scorzoni L *et al.* From moths to caterpillars: Ideal conditions
512   for *Galleria mellonella* rearing for in vivo microbiological studies. *Virulence*
513   2018;**9**:383–9.

514   Junqueira JC. *Galleria mellonella* as a model host for human pathogens: Recent
515   studies and new perspectives. *Virulence* 2012;**3**, DOI: 10.4161/viru.22493.

516   Lavine MD, Strand MR. Insect hemocytes and their role in immunity. *Insect*
517   *Biochemistry and Molecular Biology*. Vol 32. Pergamon, 2002, 1295–309.

518   Lee KA, Lee WJ. Immune–metabolic interactions during systemic and enteric
519   infection in *Drosophila*. *Curr Opin Insect Sci* 2018;**29**:21–6.

520   Leuko S, Raivio TL. Mutations that impact the enteropathogenic *Escherichia coli* Cpx
521   envelope stress response attenuate virulence in </i>Galleria mellonella<i>.
522   *Infect Immun* 2012;**80**:3077–85.

523   Li Y, Spiropoulos J, Cooley W *et al.* Galleria mellonella - a novel infection model for
524   the *Mycobacterium tuberculosis* complex. *Virulence* 2018;**9**:1126–37.

525   Little TJ, Kraaijeveld AR. Ecological and evolutionary implications of immunological
526   priming in invertebrates. *Trends Ecol Evol* 2004;**19**:58–60.

527   Liu B, Zheng Y, Yin F *et al.* Toll Receptor-Mediated Hippo Signaling Controls Innate
528   Immunity in *Drosophila*. *Cell* 2016;**164**:406–19.

529   Luther MK, Arvanitis M, Mylonakis E *et al.* Activity of daptomycin or linezolid in
530   combination with rifampin or gentamicin against biofilm-forming *Enterococcus*
531   *faecalis* or *E. faecium* in an in vitro pharmacodynamic model using simulated
532   endocardial vegetations and an *in vivo* sur. *Antimicrob Agents Chemother*
533   2014;**58**:4612–20.

534   Maguire R, Duggan O, Kavanagh K. Evaluation of *Galleria mellonella* larvae as an in
535   vivo model for assessing the relative toxicity of food preservative agents. *Cell*
536   *Biol Toxicol* 2016;**32**:209–16.

537   Mannala GK, Koettnitz J, Mohamed W *et al.* Whole-genome comparison of high and
538   low virulent *Staphylococcus aureus* isolates inducing implant-associated bone

539   infections. *Int J Med Microbiol* 2018;**308**:505–13.

540   Mowlds P, Kavanagh K. Effect of pre-incubation temperature on susceptibility of
541   *Galleria mellonella* larvae to infection by *Candida albicans*. *Mycopathologia*
542   2008;**165**:5–12.

543   Mylonakis E, Moreno R, El Khoury JB *et al. Galleria mellonella* as a model system to
544   study *Cryptococcus neoformans* pathogenesis. *Infect Immun* 2005;**73**:3842–50.

545   Olsen RJ, Ebru Watkins M, Cantu CC *et al.* Virulence of serotype M3 group A
546   *Streptococcus* strains in wax worms (*Galleria mellonella* larvae). *Virulence*
547   2011;**2**:111.

548   Peleg AY, Jara S, Monga D *et al. Galleria mellonella* as a model system to study
549   *Acinetobacter baumannii* pathogenesis and therapeutics. *Antimicrob Agents*
550   *Chemother* 2009;**53**:2605–9.

551   Ramarao N, Nielsen-Leroux C, Lereclus D. The insect *Galleria mellonella* as a
552   powerful infection model to investigate bacterial pathogenesis. *J Vis Exp* 2012,
553   DOI: 10.3791/4392.

554   Ratcliffe NA. Invertebrate immunity - A primer for the non-specialist. *Immunol Lett*
555   1985;**10**:253–70.

556   Reeves EP, Messina CGM, Doyle S *et al.* Correlation between gliotoxin production
557   and virulence of *Aspergillus fumigatus* in *Galleria mellonella*. *Mycopathologia*
558   2004;**158**:73–9.

559   Sadd BM, Schmid-Hempel P. Insect Immunity Shows Specificity in Protection upon
560   Secondary Pathogen Exposure. *Curr Biol* 2006;**16**:1206–10.

561   Salem HM, Hussein MA, Hafez SE *et al.* Ultrastructure changes in the haemocytes
562   of *Galleria mellonella* larvae treated with gamma irradiated *Steinernema*
563   *carpocapsae* BA2. *J Radiat Res Appl Sci* 2014;**7**:74–9.

564   Schell MA, Lipscomb L, DeShazer D. Comparative genomics and an insect model
565   rapidly identify novel virulence genes of *Burkholderia mallei*. *J Bacteriol*
566   2008;**190**:2306–13.

567   Seed KD, Dennis JJ. Development of *Galleria mellonella* as an alternative infection

568   model for the *Burkholderia cepacia* complex. *Infect Immun* 2008;**76**:1267–75.

569   Sheehan G, Dixon A, Kavanagh K. Utilization of *Galleria mellonella* larvae to
570   characterize the development of *Staphylococcus aureus* infection. *Microbiol
571   (United Kingdom)* 2019;**165**:863–75.

572   Singkum P, Suwanmanee S, Pumeesat P *et al.* A powerful in vivo alternative model
573   in scientific research: *Galleria mellonella*. *Acta Microbiol Immunol Hung*
574   2019;**66**:31–55.

575   Smitten KL, Southam HM, de la Serna JB *et al.* Using Nanoscopy To Probe the
576   Biological Activity of Antimicrobial Leads That Display Potent Activity against
577   Pathogenic, Multidrug Resistant, Gram-Negative Bacteria. *ACS Nano*
578   2019;**13**:5133–46.

579   The World Health Organisation. *Global Priority List of Antibiotic-Resistant Bacteria to
580   Guide Research, Discovery, and Development of New Antibiotics.*, 2017.

581   Tojo S, Naganuma F, Arakawa K *et al.* Involvement of both granular cells and
582   plasmatocytes in phagocytic reactions in the greater wax moth, *Galleria
583   mellonella*. *J Insect Physiol* 2000;**46**:1129–35.

584   Trevijano-Contador N, Zaragoza O. Immune response of *Galleria mellonella* against
585   human fungal pathogens. *J Fungi* 2019;**5**, DOI: 10.3390/jof5010003.

586   Tsai CJ-YY, Loh JMS, Proft T. *Galleria mellonella* infection models for the study of
587   bacterial diseases and for antimicrobial drug testing. *Virulence* 2016;**7**:214–29.

588   Tzompa-Sosa DA, Yi L, van Valenberg HJF *et al.* Insect lipid profile: Aqueous versus
589   organic solvent-based extraction methods. *Food Res Int* 2014;**62**:1087–94.

590   Vogel H, Altincicek B, Glöckner G *et al.* A comprehensive transcriptome and
591   immune-gene repertoire of the lepidopteran model host *Galleria mellonella*.
592   *BMC Genomics* 2011;**12**, DOI: 10.1186/1471-2164-12-308.

593   Wand ME, McCowen JWI, Nugent PG *et al.* Complex interactions of *Klebsiella
594   pneumoniae* with the host immune system in a *Galleria mellonella* infection
595   model. *J Med Microbiol* 2013;**62**:1790–8.

596   Wojda I, Taszłow P. Heat shock affects host-pathogen interaction in *Galleria*

597   *mellonella* infected with *Bacillus thuringiensis*. *J Insect Physiol* 2013;**59**:894–
598   905.

599   Wu G, Zhao Z, Liu C *et al.* Priming *Galleria mellonella* (Lepidoptera: Pyralidae)
600   Larvae With Heat-Killed Bacterial Cells Induced an Enhanced Immune
601   Protection Against *Photorhabdus luminescens* TT01 and the Role of Innate
602   Immunity in the Process. *J Econ Entomol* 2014;**107**:559–69.

603   Zasloff M. Antimicrobial peptides of multicellular organisms. *Nature* 2002;**415**:389–
604   95.

605

Supplementary

Table S1. Summary of experimental design utilised for *G. mellonella* experiments. Table adapted from Andrea, Krogfelt and Jenssen (2019) to include details of strains and a brief summary of their characteristics. (LP, left pro-leg; NA, not available, P-, privately purchased larvae from country specified).

S. aureus strain	Strain characteristics	Larval weight/size	Larval origin	Storage	Injection site	Infection	Reference
EDCC 5455-5461	clinical isolates	150–200 mg	Reared	30°C	Not given	1.0 x10^6	(Mannala *et al.* 2018)
EDCC 5464	clinical isolate, MRSA strain						
RN4220		NA	P-UK	4°C	Between segments	~1.3 x10^6	(Ba *et al.* 2015)
LGA251	veterinary isolate, *mecC* positive						
02.5099.D	clinical isolate, *mecC* positive						
ATCC 43300	MRSA, type culture	15–25 mm long	P-UK	7 days	LP	0.8–2.6 x10^6	(Bazaid *et al.* 2018)
Newman							
NCTC 13277	MRSA, type culture						
2x clin. isol.							
ATCC 29213	MSSA	~250 mg	P-China	NA	LP	~1.0 x10^6	(Dong *et al.* 2017)
ATCC 43300	MRSA						
N54	MSSA, clinical isolate						
MRSA N9	MRSA, clinical isolate						
USA300 JE2	MRSA	300–700 mg	P-Netherlands	NA	LP	1.0 x10^6	(Ebner *et al.* 2016)
ATCC 25923	type culture	~200 mg	NA	NA	LP	1.0 x10^3	(Ferro *et al.* 2016)
ATCC 6538	type culture						
SA01-04	clinical isolates						
USA300-0114		200–300 mg	P-USA	4°C, 14 days	LP	5.0 x10^6	(Jacobs *et al.* 2013)
UAMS-1							
UAMS-1112							
RN4220							
ATCC 6538	type culture	NA	Reared	28°C	NA	10^8 CFU/ml	(Jorjão *et al.* 2018)
ATCC 11195	MSSA, type culture	NA	P-UK	4°C, 14 days	NS	~2.5 x10^6	(Gibreel and Upton 2013)

Table S2. Multiple comparison results for change in lipid weight 24 h post-MRSA infection described in Figure 5. (PBS; phosphate-buffered saline injection; NM, no manipulation control)

Interaction	Mean rank diff.	Adjusted *p-value*	Summary
NM vs. PBS	78.87	>0.9999	ns
NM vs. Live	339.5	<0.0001	****
NM vs. Dead	490.7	<0.0001	****
PBS vs. Live	260.6	<0.0001	****
PBS vs. Dead	411.8	<0.0001	****
Live vs. Dead	151.2	<0.0001	****

Table S3. Editable excel table that can be used in order to calculate the LD50 for MRSA based on weight-grouping.

Calculating the LD50 for MRSA NCTC 12493

Equation as given by linear model: **y = 0.007966x + 5.548**

Larvae weight (mg): **x =**	*180*	*Insert here the median weight for the selected weight group*
LD_{50} (Log[CFU/mg]): **y =**	**9.61E+06**	This is the LD_{50} for your selected weight group
LD_{50} (CFU):	**2.88E+09**	This is the total density of MRSA 12493 that must be injected into larva of the selected weight-group in order to kill 50% of the population